Bioorganic & Medicinal Chemistry Letters 29 (2019) 126604

Contents lists available at ScienceDirect

Bioorganic & Medicinal Chemistry Letters

journal homepage: www.elsevier.com/locate/bmcl

Structure based design of macrocyclic factor XIa inhibitors: Discovery of cyclic P1 linker moieties with improved oral bioavailability

Charles G. Clark*, Karen A. Rossi, James R. Corte, Tianan Fang, Joanne M. Smallheer, Indawati De Lucca, David S. Nirschl, Michael J. Orwat, Donald J.P. Pinto, Zilun Hu, Yufeng Wang, Wu Yang, Yoon Jeon, William R. Ewing, Joseph E. Myers Jr., Steven Sheriff, Zhen Lou, Jeffrey M. Bozarth, Yiming Wu, Alan Rendina, Timothy Harper, Joanna Zheng, Baomin Xin, Qian Xiang, Joseph M. Luettgen, Dietmar A. Seiffert, Ruth R. Wexler, Patrick Y.S. Lam

Bristol-Myers Squibb Company, P.O. Box 4000, Princeton, NJ 08543, United States

ARTICLE INFO

Keywords:
Factor XIa inhibitors
FXIa
Activated partial thromboplastin time
aPTT
Thrombosis
Anticoagulant
Bioavailability

ABSTRACT

This manuscript describes the discovery of a series of macrocyclic inhibitors of FXIa with oral bioavailability. Assisted by structure based drug design and ligand bound X-ray crystal structures, the group linking the P1 moiety to the macrocyclic core was modified with the goal of reducing H-bond donors to improve pharmacokinetic performance versus **9**. This effort resulted in the discovery of several cyclic P1 linkers, exemplified by **10**, that are constrained mimics of the bioactive conformation displayed by the acrylamide linker of **9**. These cyclic P1 linkers demonstrated enhanced bioavailability and improved potency.

Cardiovascular disease (CVD) and stroke cause extensive economic strain on society and are the leading cause of death worldwide.[1] As of 2013, within the US alone, one out of every three deaths could be attributed to some form of CVD despite the numerous strategies that exist to reduce morbidity and mortality by improving or preserving good cardiovascular health.[2] Antithrombotic agents offer a well proven option for treatment and prevention.[3] Warfarin, a decades old agent for thromboembolic disease management, has a narrow therapeutic index that requires frequent monitoring, and its inhibition is non-specific. These drawbacks focused attention on the need for the discovery and development of safer and more easily managed medicines.[4] Within the past decade novel oral anticoagulants (NOACS), which act as inhibitors of thrombin or the coagulation factor Xa (FXa), have provided improved benefits in the treatment or prevention of DVT (deep vein thrombosis), PE (pulmonary embolism) and stroke arising from non-valvular atrial fibrillation (NVAF).[5]

Coagulation factor XIa (FXIa) offers a newer target in antithrombotic therapy.[6] In the classic waterfall model, FXIa lies upstream in the intrinsic pathway, and inhibition may provide protection from thrombosis while limiting bleeding risk. This is supported by the demonstrated efficacy of small molecule FXIa inhibitors in multiple animal thrombosis models without a significant effect on bleeding time.[7] Moreover, clinical evidence from a FXI antisense oligonucleotide showed a decreased occurrence of DVT during knee replacement surgery, without increasing the number of bleeding events versus enoxaparin.[8]

As part of our program to discover FXIa inhibitors amenable to oral dosing, we previously disclosed potent phenylimidazole compounds,[9] exemplified by **1**,[10,11] which while potent and selective, exhibit low oral bioavailability.

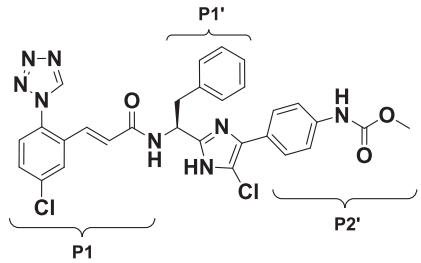

1
FXIa Ki = 5.8 nM
aPTT $EC_{1.5x}$ = 5.2 μM
rat PK: F = 3%
PSA: 140 Å^2

In this communication we describe the use of structure-based drug design and ligand bound X-ray crystal structures that led to the

* Corresponding author.
E-mail address: charles.clark@bms.com (C.G. Clark).

https://doi.org/10.1016/j.bmcl.2019.08.008
Received 23 May 2019; Received in revised form 30 July 2019; Accepted 4 August 2019
Available online 16 August 2019
0960-894X/

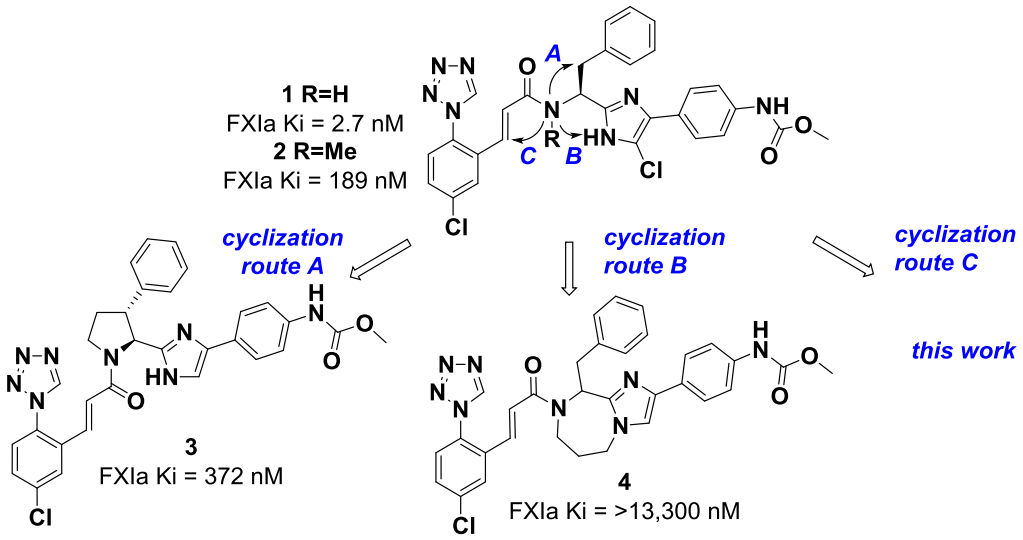

Fig. 1. Amide hydrogen remval strategies for **1**. K_i values shown were obtained at 25 °C.

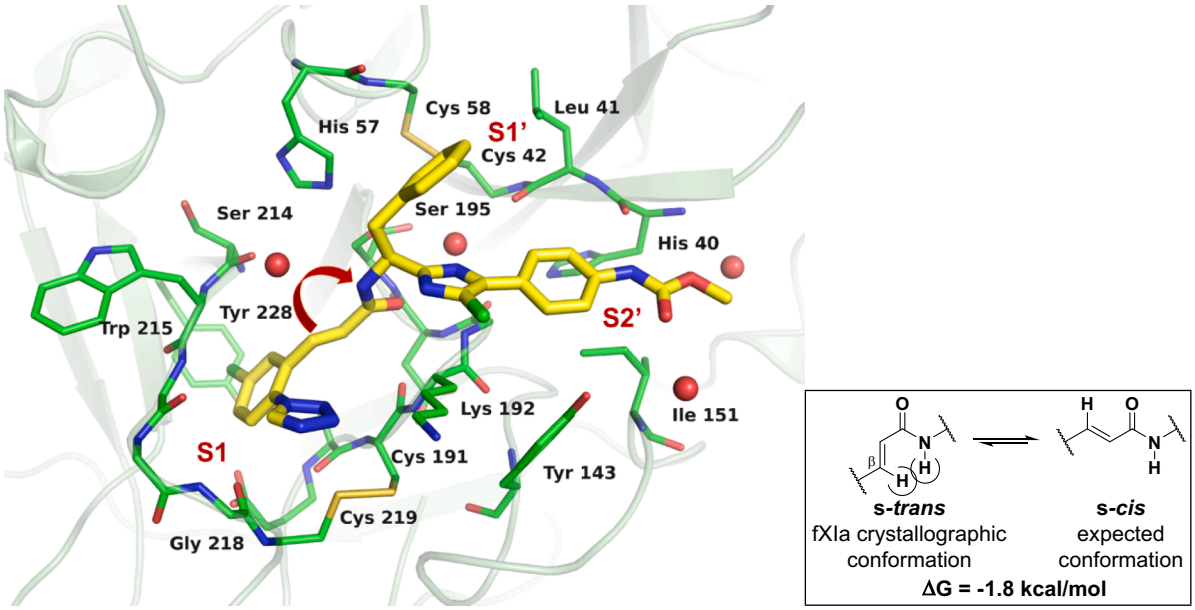

Fig. 2. X-ray crystal of **1** bound to FXIa with red arrow indicating potential point of conformational constraint. The red spheres represent water molecules.

discovery of a series of FXIa inhibitors with novel P1 linkers that have greatly enhanced bioavailability and improved potency. To improve the permeability and oral absorption of compounds represented by **1**, the number of hydrogen bond donors/acceptors and the polar surface area (PSA) were reduced.[12] The amide hydrogen and the tetrazole moiety, which were responsible for 31% of the total PSA, were eliminated.[13] Since removal of the tetrazole resulted in a significant loss in FXIa activity,[10] the aim was to lower the conformational energy by modifying the acrylamide linker in a fashion that would pre-organize the system towards the bioactive conformation. Moreover, rigidifying a molecule through removal of rotatable bonds has been shown to have a positive effect on permeability.[14,15]

Previous attempts towards removing the amide hydrogen of **1** via *N*-alkylation, in the case of **2**, or by tying back to either the benzylic methylene (cyclization route A to give **3**) or to the imidazole (cyclization route B to give **4**) were not successful with respect to maintaining FXIa activity (Fig. 1). Therefore an alternate cyclization strategy (cyclization route C), which incorporates a conformational constraint between the amide nitrogen and the acrylamide linker, was designed.

Evaluation of the FXIa protein bound crystal structure of **1**[16] indicated an eclipsed nature of the amide proton with the β-proton of the acrylamide (Fig. 2). This bound conformation exists in a slightly strained s-*trans* orientation (Fig. 2 inset),[17] and suggested the potential for constraint via cyclization as indicated by the red arrow. The s-*trans* conformation was unexpected as the vast majority of acyclic aliphatic acrylamides found in the Cambridge Structural Database (109 out of 111) exist in the s-*cis* conformation.

Based on this observation a variety of cyclic linker motifs were designed. These motifs were prioritized with the aid of molecular modelling and synthesized on the chemotype of **1** removing the tetrazole moiety to improve permeability. The 6-membered cyclic urea **7** and cyclic carbamate **8**[18] were found to maintain or improve fXIa affinity versus the acyclic urea and amide analogs **5** and **6** (Fig. 3).

Incorporation of the cyclic carbamate into our previously described 13-membered macrocyclic FXIa inhibitors[19] provided a 78-fold gain in FXIa affinity in **10**[20] as compared to the linear analog **8** (Fig. 4). A 33-fold gain in FXIa affinity was also observed when the acrylamide moiety of **9** was replaced in **10** by the cyclic carbamate, as compared to the

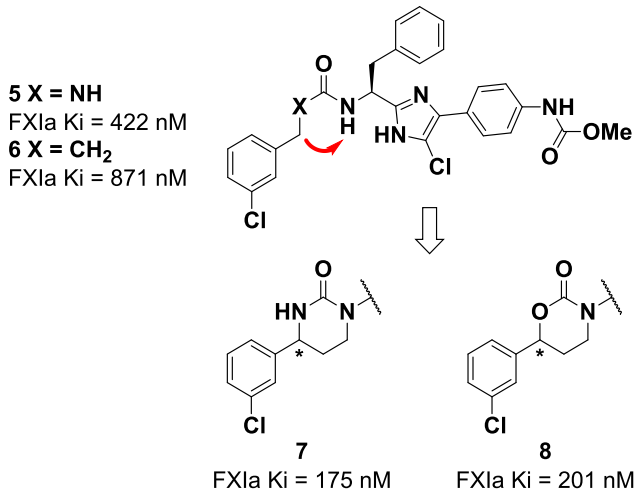

Fig. 3. Most active P1 cyclic linkers from initial screen. K_i values shown were obtained at 25 °C.

more moderate gain obtained with the linear imidazole compounds shown in Fig. 3. The epimer **11** was less active with respect to both FXIa affinity and *in vitro* anticoagulant activity (aPTT). Macrocyclic amide **10** met our targeted molecular properties goal of PSA < 130 Å^2, while minimizing the total number of H-bond donors and rotatable bonds.[21]

The urea and lactam linkers when incorporated in the macrocylic series (**12**[22] and **13**,[23] Table 1), also displayed both enhanced FXIa affinity and aPTT activity. Fluoro substitution on the phenyl ring, previously shown to further enhance activity,[19,24] resulted in a 2–3 fold improvement in both FXIa affinity and aPTT activity in compounds **14–16**. Liver microsome (LM) stability for carbamate **14** and lactams **13** and **16** was determined to be low as compared to the ureas **12** and **15** and acrylamide **9**.[25] In an attempt to remedy the low metabolic stability, the linker carbon atom was replaced with a nitrogen as in piperazinone **17**, which resulted in significantly reduced FXIa affinity versus **13**.

A comparison of the FXIa-bound crystal structures of cyclic carbamate **10** and the corresponding acrylamide **18**[19] show that they bind in nearly identical conformations (Fig. 5), such that the P1 phenyl moiety of each nearly superimposes. Interpretation of the crystal structure of **10** suggests that maintaining a hydrogen on the atom alpha to the carbonyl (i.e., methylene in the case of the lactam and NH in the case of the urea) could be beneficial in order to interact with the carbonyl of Cys191 (distance 3.2 Å) and could account for the slightly greater activity observed for the lactam and urea chemotypes versus the (*R*)-carbamate.

Table 1
Cyclic linker modifications in the 13-membered macrocycles.

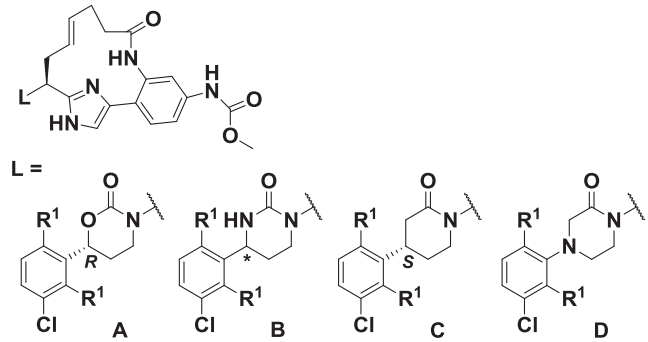

Compd #	L	R^1	FXIa Ki (nM)	aPTT $EC_{1.5x}$ (μM)	LM[a] $t_{1/2}$ (min) H, R
10	A	H	17	5.9	NT
12	B	H	4.8	3.7	35, 18
13	C	H	5.3	3.0	6, 5
14	A	F	4.7	2.0	8, 15
15	B	F	1.8	1.8	41, 26
16	C	F	2.2	1.4	9, 7
17	D	H	333	> 40	15, NT

[a] LM = liver microsome stability half-life in minutes for human (H) & rat (R).

To further explore the cyclic linker series, substituents on the P1 phenyl and cyclic carbamate ring were varied (Table 2). Transitioning into the more potent chloro imidazole series (X = Cl) yielded a gain in FXIa affinity and aPTT potency similar to earlier disclosed compounds.[10,19] Addition of a 6-fluoro substitution on the P1 phenyl in **20** showed a modest improvement in FXIa affinity. Compound **21** with a 3-chloro-2-fluoro-6-trifluoromethyl phenyl P1 group had similar FXIa Ki and aPTT to compound **20.** The 2,6-di-fluoro analog **22**[26] gained FXIa affinity and aPTT activity versus the mono-F analog **20**; however, LM stability remained poor. Since the benzylic position (R^3) could serve as a potential metabolic soft spot, an attempt to improve LM stability in this series was explored. The deutero analog **23** was prepared in an attempt to improve the microsomal stability. While it showed a 3-fold gain in Ki and 2-fold gain in aPTT, no significant change in liver microsome stability was observed.

The PK profiles of two of the three types of P1 linkers, cyclic carbamate **10** and lactam **13,** plus the acrylamide, represented by compounds **9** and **18**, were evaluated in a rat PK study, the results of which are summarized in Table 3. Compound **9** exhibited high clearance, a

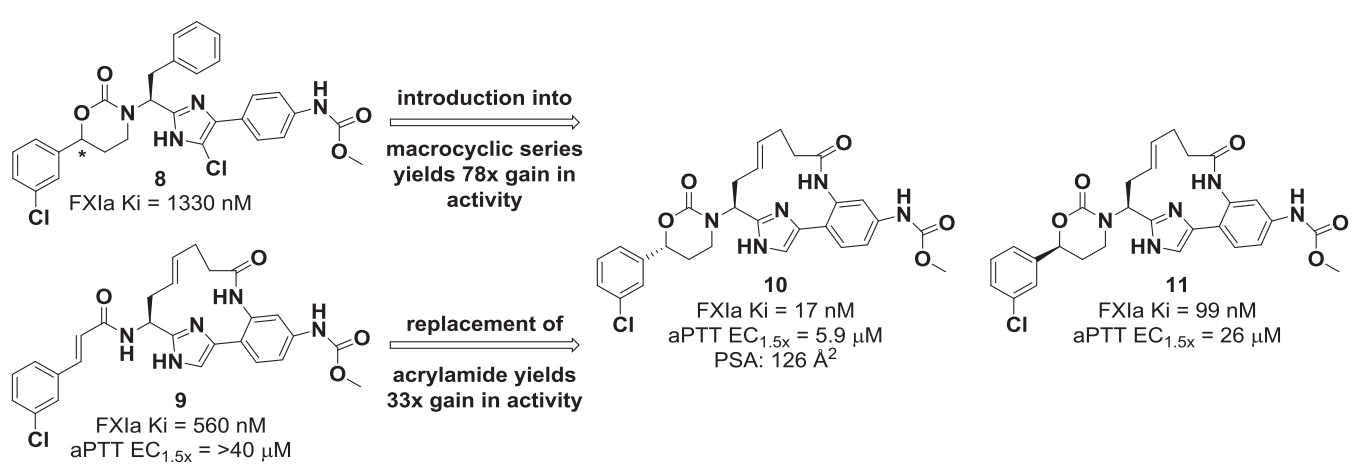

Fig. 4. Introduction of cyclic linker into macrocyclic amide series leading to discovery of **10**. Comparison of cyclic carbamate epimers **10** and **11**.

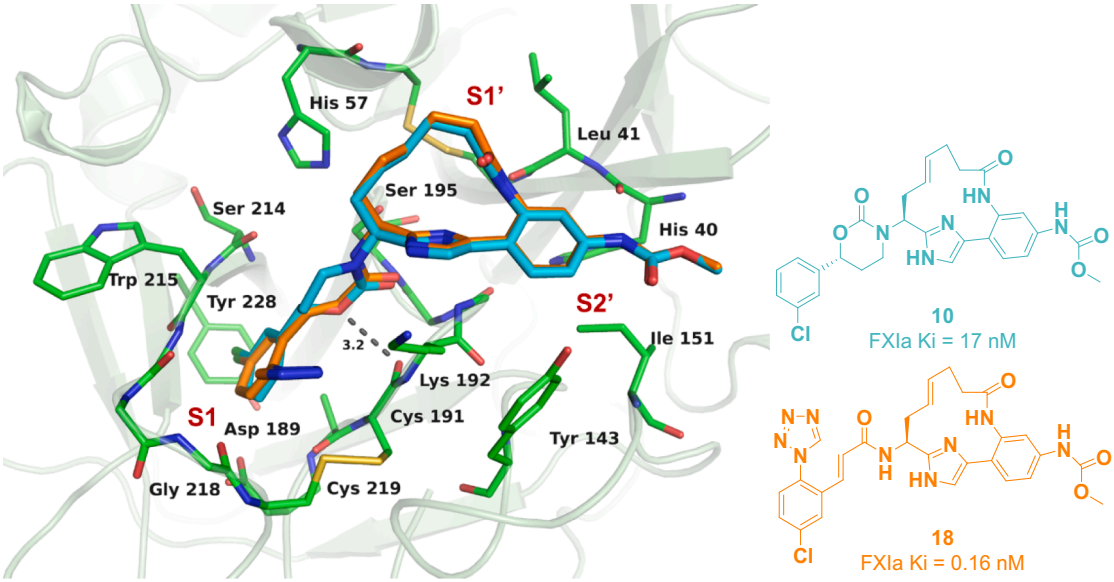

Fig. 5. Overlay of X-ray crystal structures of cyclic carbamate **10** (cyan) and chlorophenyl tetrazole acrylamide **18** (gold) bound to FXIa. The dotted line indicates a potential H-bond from the position alpha to the carbonyl to the oxygen of Cys191.

Table 2
Modification to P1 phenyl and cyclic carbamate in 13-membered macrocycle.

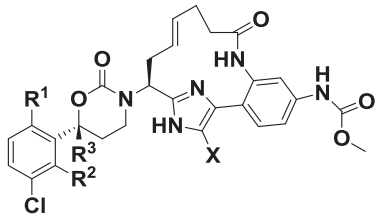

Compd #	R^1	R^2	R^3	X	FXIa Ki (nM)	aPTT $EC_{1.5x}$ (μM)	LM[a] $t_{1/2}$ (min) H, R
10	H	H	H	H	17	5.9	NT
19	H	H	H	Cl	4.4	2.6	11, 14
20	F	H	H	Cl	2.1	1.9	5, 18
21	CF_3	F	H	Cl	1.8	2.4	18, 49
22	F	F	H	Cl	0.95	0.91	9, 22
23	F	F	D	Cl	0.27	0.45	16, 31

[a] LM = liver microsome stability half-life in minutes for human (H) & rat (R).

half-life of 1.4 hr, and oral bioavailability of 2%. Cyclic carbamate **10**[27] also displayed high clearance, but had a reduced steady state volume of distribution (Vd_{ss}), a shorter half-life, and significant improvement in oral bioavailability (F% = 59). Lactam **13** was shown to have clearance

Table 4
Human serine protease selectivity profile for **10**.

Human Enzyme Ki (nM)[a]	**10**	**13**
Factor XIa	17	5.3
Factor VIIa[b]	> 13,300	4850
Factor IXa	> 27,100	> 27,100
Factor Xa[b]	3660	> 9,000
Factor XIIa	> 3,050	> 3050
Thrombin[b]	> 13,300	> 13,300
Trypsin[b]	6,260	> 6,260
Activated Protein C	> 21,500	> 7,160
Plasmin	> 15,200	> 15,200
TPA	> 6,150	> 6,150
Urokinase	> 15,100	> 15,100

[a] K_i values in nM were obtained using human purified enzymes at 37 °C.
[b] K_i values in nM were obtained using human purified enzymes at 25 °C.

well above hepatic blood flow and a shortened half-life with modest oral bioavailability. Compound **18** displayed medium clearance, a reduced Vd_{ss}, a shorter half-life, and oral bioavailability of 0.8%.

Compound **10** was tested across a number of coagulation related human serine proteases and trypsin showing at least several hundred fold selectivity (Table 4).

Cyclic carbamate compounds **10** and **11** were synthesized as shown in Scheme 1 starting from commercially available 3-chlorobenzaldehyde **24**. Addition of vinyl magnesium bromide to the aldehyde at −78 °C provided vinyl alcohol **25,** which was then oxidized

Table 3
Pharmacokinetic profile of selected compounds in rat studies.

Compd #	FXIa Ki (nM)	aPTT $EC_{1.5x}$ (μM)	LM $t_{1/2}$ (min) H, R	Caco-2 AB/BA (nm/s)	AUC (nM*h)	Dose IV/PO (mpk)	Cl[a] (mL/min/kg)	Vd_{ss} (L/kg)	$T_{1/2}$ (h)	F (%)	PSA (Å^2)
9	560	> 40	32, 45	< 15/324	27	0.52/1.04[b]	44	3.2	1.4	2	125
10	17	5.9	NT[d]	NT	523	0.68/1.36[b]	40	1.3	0.8	59	126
13	5.3	2.9	6, 5	46/309	31	0.63/1.27[c]	188	4.6	0.5	15	116
18	0.16	0.27	41, 39	< 15/58	11	0.79/1.58[b]	28	0.7	0.7	0.8	169

[a] Vehicle for iv and po: 70% PG; 20% water; 10% ethanol.
[b] Compound was dosed in a cassette format.
[c] Compound was dosed in a discrete format.
[d] See footnote 27.

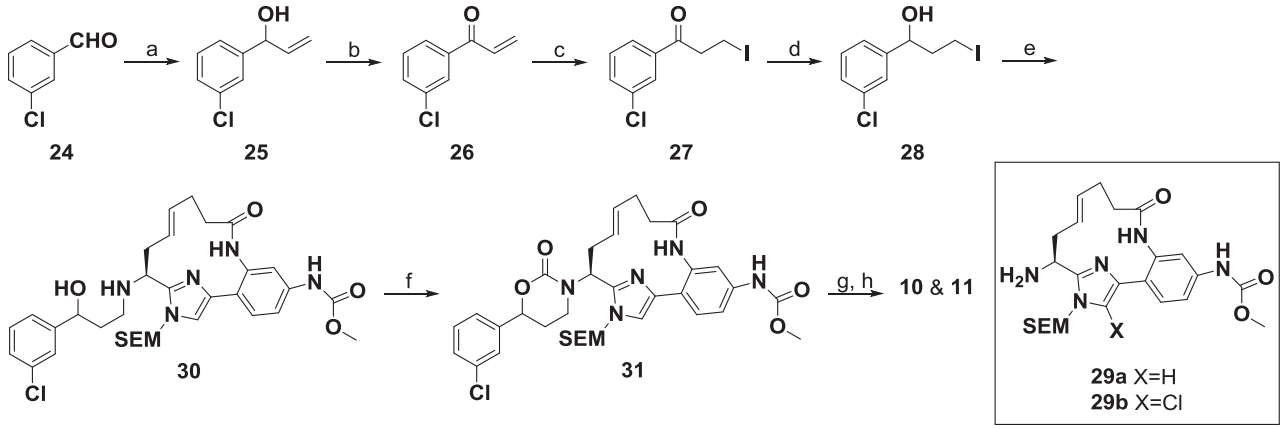

Scheme 1. Reagents and conditions: (a) vinylmagnesium bromide, THF, −78 °C to rt, > 90%; (b) CrO_3, H_2SO_4 (aq.), acetone, 0 °C to rt, > 90%; (c) TMSCl, NaI, H_2O, MeCN, > 90%; (d) $NaBH_4$, H_2O, THF; (e) **29a**, K_2CO_3, MeCN, 80 °C, 41%; (f) CDI, TEA, dioxane, 110 °C, 56%; (g) 4 M HCl, dioxane, 75 °C, 54%; (h) prep chiral SFC to separate isomers.

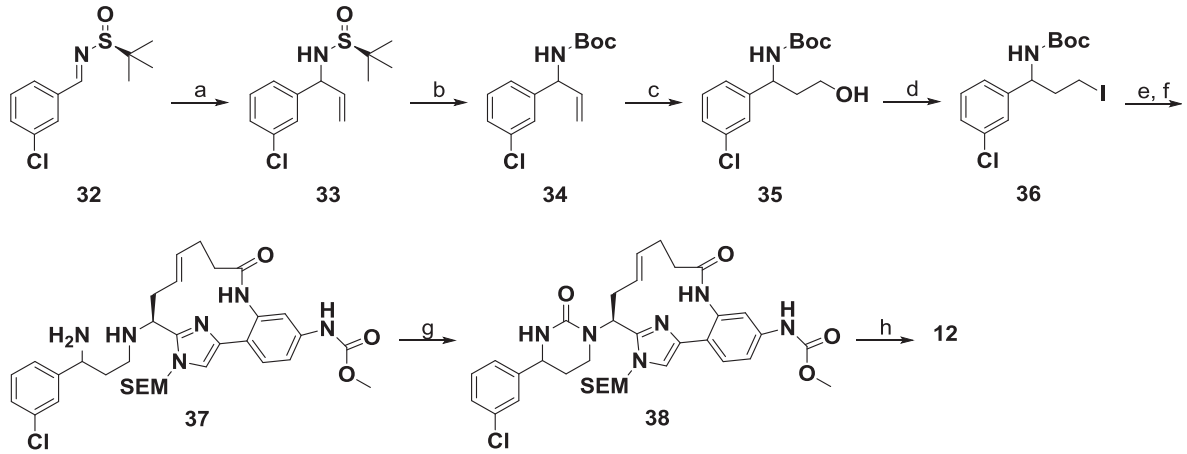

Scheme 2. Reagents and conditions: (a) vinylmagnesium bromide, THF, −78 °C to rt, 73% (23% de); (b) 4 M HCl in dioxane then Boc_2O, TEA, MeCN, 40% over two steps; (c) 9-BBN, THF, 100 °C, then H_2O_2, NaOH, EtOH, 45 °C, 73%; (d) MsCl, DIPEA, DCM, then NaI, acetone, reflux, 81%; (e) **29a**, K_2CO_3, MeCN, 75 °C; (f) 20% TFA, DCM, 37% over 2 steps; (g) CDI, THF, 67%; (h) 4 M HCl, dioxane, 75 °C, then preparatory reverse phase HPLC to separate isomers, 22%.

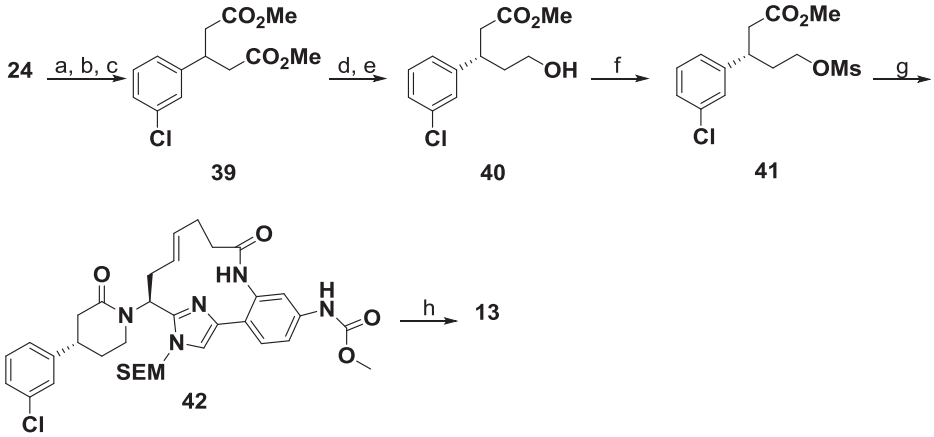

Scheme 3. Reagents and conditions: (a) methyl acetoacetate, piperidine, MeOH; (b) NaOMe, reflux; (c) HCl, MeOH, reflux, 52% over three steps; (d) NaOH, MeOH (e) BH_3·DMS, 64% over two steps, then preparatory chiral SFC to separate enantiomers; (f) MsCl, TEA, DCM, 0 °C, 89%; (g) **29a**, DIPEA, PhMe, 150 °C, 18%; (h) 4 M HCl, dioxane, 65 °C, 35%.

with Jones reagent to the corresponding vinyl ketone **26.** Addition of HI, generated in situ from NaI and TMSCl, by the method of Irifune et al.,[28] to the double bond gave the iodoketone **27,** which was then reduced with $NaBH_4$ to the racemic iodoalcohol **28**. Alternatively, iodoketone **27** can be reduced using (*S*)-CBS reagent[29] to yield the (*R*)-iodo-alcohol **28** in > 90% yield and 60–70% ee. Alkylation of macrocyclic amine **29a** with iodide **28** in the presence of K_2CO_3 in acetonitrile at 80 °C provided the aminoalcohol intermediate **30**. Cyclization by treatment with CDI and TEA in refluxing dioxane provided cyclic carbamate **31.** Removal of the SEM protecting group from the imidazole and chiral separation afforded **10** and **11**.

Compounds **14**, and **19–22** were similarly synthesized by substituting the appropriately substituted benzaldehyde starting material for **24** and the applicable macrocyclic amine **29a-b** to generate the desired compounds. Compound **23** was synthesized by use of $NaBD_4$ to reduce the appropriately substituted ketone **27** to a deutero-analog of

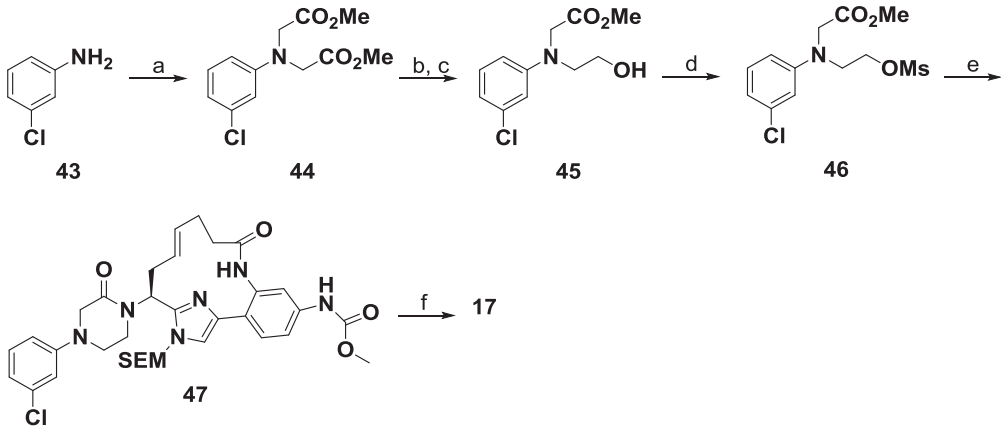

Scheme 4. Reagents and conditions: (a) methyl 2-bromoacetate, K_2HPO_4, KI, MeCN, reflux, 48%; (b) NaOH, MeOH (c) BH_3·DMS, 34% over two steps; (d) MsCl, pyridine, DCM, 0 °C, 100%; (e) **29a**, DIPEA, PhMe, 120 °C, 20%; (f) 4 M HCl, dioxane, 75 °C, 28%.

31, which was then used in the same fashion as shown in Scheme 1.

The cyclic urea compound **12** was synthesized as shown in Scheme 2 starting from commercially available (*S*)-N-(3-chlorobenzylidene)-2-methylpropane-2-sulfinamide **32**. Addition of vinyl magnesium bromide to the sulfinimine at −78 °C provided the 1-allyl sulfinamide **33** in 23% de. Removal of the chiral auxillary with HCl and protection of the amine with Boc_2O yielded *N*-allyl Boc-amine **34,** which was hydroborated using 9-BBN, and the intermediate oxidized with H_2O_2 to give the Boc-protected amino alcohol **35**. Treatment of **35** with mesyl chloride followed by NaI in refluxing acetone provided the protected amino iodide **36.** This intermediate iodide **36** was used to alkylate macrocyclic amine **29a** in the presence of K_2CO_3 in acetonitrile at 75 °C, followed by treatment with TFA to furnish the diamine **37**. Cyclization by treatment with CDI in THF at ambient temperature provided cyclic urea **38.** Subsequent removal of the SEM protecting group from the imidazole and reverse phase HPLC separation of the diastereomeric isomers afforded **12**. Compound **15** was similarly synthesized by substituting (*S*)-N-(3-chloro-2,6-difluorobenzylidene)-2-methylpropane-2-sulfinamide for **32** and the macrocyclic amine **29a** to generate the desired compound.

Lactam **13** was synthesized as shown in Scheme 3 starting from commercially available 3-chlorobenzaldehyde **24**. Condensation of **24** with methyl acetoacetate in the presence of piperidine gave di-ester **39**. Mono-ester hydrolysis followed by borane reduction yielded a racemic alcohol which is purified by chiral SFC to furnish (S)-alcohol **40**. Treatment with mesyl chloride gave **41** which was reacted with macrocyclic amine **29a** in the presence of Hunig's base in toluene at 150 °C to effect sequential alkylation and ring-closing condensation to provide SEM-protected lactam **42**. Subsequent removal of the SEM protecting group from the imidazole afforded **13**. Compound **16** was similarly synthesized by substituting 3-chloro-2,6-difluorobenzaldehyde for **24** and the applicable macrocyclic amine **29b**.

The piperazinone **17** was synthesized as shown in Scheme 4 starting from commercially available 3-chloroaniline **43**. Bis-alkylation of **43** generated di-ester **44** which underwent mono-ester hydrolysis and borane reduction to yield alcohol **45**. Treatment with mesyl chloride gave **46** which was reacted with macrocyclic amine **29a** in the presence of Hunig's base in toluene at 120 °C to effect sequential alkylation and ring-closing condensation to provide SEM-protected piperazinone **47**. Subsequent removal of the SEM protecting group from the imidazole afforded **17**.

In conclusion, a novel series of FXIa inhibitors with cyclic P1 linkers was designed based on the X-ray crystal structure of **1**. By constraining the P1 linker into a variety of cyclic structures, we were able to maintain the bioactive conformation and good overall FXIa affinity, while removing the tetrazole moiety and acrylamide proton, both presumed to be responsible for impairing good oral bioavailability. The cyclic carbamate **10** was evaluated in a rat pharmacokinetic model and found to impart a significant increase in oral bioavailability.

Acknowledgements

The authors thank Atsu Apedo and Douglas B. Moore for chiral separations. Use of the Advanced Photon Source was supported by the U. S. Department of Energy, Office of Science, Office of Basic Energy Sciences, under Contract No. DE-AC02-06CH11357. Use of the IMCA-CAT beamline 17-ID at the Advanced Photon Source was supported by the companies of the Industrial Macromolecular Crystallography Association through a contract with Hauptman-Woodward Medical Research Institute.

References

1. Wang H, et al. Global, regional, and national life expectancy, all-cause mortality, and cause-specific mortality for 249 causes of death, 1980–2015: a systematic analysis for the Global Burden of Disease Study 2015. *Lancet.* 2016;388:1459–1544.
2. ISTH Steering Committee for World Thrombosis Day. Thrombosis: a major contributor to the global disease burden. *J Thromb Haemost.* 2014;12:1580–1590.
3. Gulpen AJW, Ten Cate-Hoek AJ, Ten Cate H. Upstream versus downstream thrombin inhibition. *Exp Rev Cardiovasc Ther.* 2016;14:1273–1282.
4. Hawkins D. Limitations of traditional anticoagulants. *Pharmacotherapy.* 2004;24:62S–65S.
5. Yeh CH, Hogg K, Weitz JI. Overview of the new oral anticoagulants: opportunities and challenges. *Arterioscler Thromb Vasc Biol.* 2015;35(5):1056–1065.
6. Gailani D, Gruber A. Factor XI as a therapeutic target. *Arterioscler Thromb Vasc Biol.* 2016;36:1316–1322.
7. (a) Wong P, Crain E, Watson C, Schumacher W. A small-molecule factor XIa inhibitor produces antithrombotic efficacy with minimal bleeding time prolongation in rabbits. *J Thromb Thrombolysis.* 2011;32:129–137;

   (b) Wong PC, Quan ML, Watson CA, et al. In vitro, antithrombotic and bleeding time studies of BMS-654457, a small-molecule, reversible and direct inhibitor of factor XIa. *J Thromb Thrombolysis.* 2015;40:416–423.
8. Büller HR, Bethune C, Bhanot S, et al. Factor XI antisense oligonucleotide for prevention of venous thrombosis. *New Engl J Med.* 2015;372:232–240.
9. Hangeland JJ, Friends TJ, Rossi KA, et al. Phenylimidazoles as potent and selective inhibitors of coagulation factor XIa with in vivo antithrombotic activity. *J Med Chem.* 2014;57:9915–9932.
10. Pinto DJ, Smallheer JM, Corte JR, et al. Structure-based design of inhibitors of coagulation factor XIa with novel P1 moieties. *Bioorg Med Chem Lett.* 2015;25:1635–1642.

11.. FXIa K_i values were obtained from purified human enzyme at 37 °C unless otherwise noted and were averaged from multiple determinations. aPTT (activated partial thromboplastin time) *in vitro* clotting assay was performed in human plasma. The reported $EC_{1.5x}$ values are the FXIa inhibitor plasma concentrations which produce a 50% increase in the clotting time relative to the clotting time in the absence of the inhibitor. Further details of both assays are described in Ref. 19.

12. Corte JR, Fang T, Pinto DJP, et al. Orally bioavailable pyridine and pyrimidine-based Factor XIa inhibitors: discovery of the methyl N-phenyl carbamate P2 prime group. *Bioorg Med Chem.* 2016;24:2257–2272.

13.. Our targeted molecular properties goal was PSA < 130 $Å^2$.

14. Veber DF, Johnson SR, Cheng H-Y, Smith BR, Ward KW, Kopple KD. Molecular properties that influence the oral bioavailability of drug candidates. *J Med Chem.*

2002;45:2615–2623.
15.. **1** has a rotatable bond count equal to 10.
16. Hu Z, Wong PC, Gilligan PJ, et al. Discovery of a potent parenterally administered factor XIa inhibitor with hydroxyquinolin-2(1H)-one as the P2' moiety. *ACS Med Chem Lett.* 2015;6:590–595.
17.. Quantum mechanical relative energy calculations of the *cis* and *trans* isomers were completed using RIMP2/cc-pVTZ//B3LYP/6-31G** with CosmoRS solvent correction.
18.. The cyclic linkers **7** and **8** shown in Fig. 3 are homochiral. Absolute stereochemistry at the starred bond connection was not determined for these compounds. The more active epimer is shown.
19. Corte JR, Fang T, Osuna H, et al. Structure-based design of macrocyclic factor XIa inhibitors: discovery of the macrocyclic amide linker. *J Med Chem.* 2017;60:1060–1075.
20.. The absolute stereochemistry of **10** was assigned based on an X-ray co-crystal (2.00 Å resolution) with FXIa. The PDB deposition number is 5QQO.
21.. The values for **10** are as follows: PSA 126 $Å^2$, H-bond donor/acceptors 9, and rotatable bonds 4.
22.. The absolute stereochemistry of the compounds in the urea linker series (**12** and **15**) were not assigned an absolute stereochemical configuration. In all cases the more active epimer is shown for comparative purposes.
23.. The absolute stereochemistry of **13** was assigned based on an X-ray co-crystal (2.08 Å resolution) with FXIa. The PDB deposition number is 5QQP.
24. Corte JR, Yang W, Fang T, et al. Macrocyclic inhibitors of Factor XIa: discovery of alkyl-substituted macrocyclic amide linkers with improved potency. *Bioorg Med Chem Lett.* 2017;27:3833–3839.
25.. Liver microsome stability was obtained for **9** and is LM t½ (min) H, R: 32, 45.
26.. Compound **22** was assayed as a diastereomerically enriched mixture at R^3.
27.. Liver microsome stability was obtained for a 1:1 mixture of **10** and **11** and is t½ (min) H, R: 11, 7.
28. Irifune S, Kibayashi T, Ishii Y, Ogawa M. A facile synthesis of alkyl iodides and deuterated alkyl iodides by hydroiodination and deuterioiodination of olefins. *Synthesis.* 1988;366.
29. Corey EJ, Reichard GA. Enantioselective and practical synthesis of *R*- and *S*-fluoxetines. *Tetrahedron Lett.* 1989;30:5207.